NASCAP CHARGING CALCULATIONS FOR A SYNCHRONOUS ORBIT SATELLITE

N. L. Sanders and G. T. Inouye
TRW Defense and Space Systems Group

INTRODUCTION

The NASA Charging Analyzer Program (NASCAP)[1] represents the state of the art in the computation of spacecraft charge up in the energetic plasma environment of geosynchronous orbits. The problem of determining the chargeup potentials of various parts of a real spacecraft in orbit is extremely complex, and the achievement of practical and useable results involves many tradeoffs between the accuracy and self-consistency of the equations solved and the manpower and computer costs. The work discussed in this paper represents the first use of NASCAP by an industrial user and is a part of an effort to eliminate the hazards of spacecraft charging to a satellite in geosynchronous orbit.

Satellite Modeling

The modeling of a geometrically complex spacecraft for the purpose of ambient plasma charging analyses was dictated by the capabilities of the NASCAP computer program. The geometrical limitations in defining the spacecraft for NASCAP are

- The spacecraft must be defined in terms of a limited number of building blocks. These are shown in Figure 1. In addition to the six building blocks shown, thin plates, such as were used to represent the solar array paddles, are included in the repertory.
- The building blocks must line up with the orthogonal coordinate system. The solar array paddles could not be tilted, for example. This is the reason for the right angle bend in the paddles.
- The total spacecraft is limited to less than 1200 surface cells.
- The spacecraft must fit into a volume of 17 x 17 x 33 unit cell dimensions.

Once the spacecraft is defined geometrically, NASCAP provides drawings whereby the definition may be validated visually. Figure 2 is a view showing the building block representation used for the satellite. Figure 3 shows the individual surface cells outlined. Each cell (there are a total of 810) characterized by its material is considered to be an equipotential surface. The unit cell dimension was assumed to be a 1 foot square making the overall dimensions somewhat comparable to the actual spacecraft.

Materials Parameters Used in the Charging Analyses

The material properties such as resistivity, photoemission, secondary emission, and backscatter coefficients have a major impact on the charging characteristics and differential potentials obtained when a spacecraft is exposed to the substorm environment. NASCAP has, within its files, 14 typical spacecraft materials characterized in terms of 13 parameters as shown in Table 1.

The 13 parameters or properties are identified in Table 2. For the satellite under study, eight of these were taken without change and a few properties such as thickness and conductivity were changed to values which were more appropriate. These eight materials are listed in Table 3 with reference to the NASCAP material selected to represent it. Also shown are the changes made in the thickness and conductivity values of Table 1. The data in Tables 1 and 2 were taken from Reference 1.

NASCAP provides drawings whereby the specifications of materials may be checked as to the locations on the spacecraft. Figure 3, as an example, shows the bottom view of the satellite model with the materials identified for each surface cell.

NASCAP Charging Analyses

The spacecraft charging analyses performed by NASCAP are complex and require a very large computer and sopnisticated programming. Even with the availability of a large computer, the computations are time consuming and limits, to 1200 surface cells, for example, are required so that computation costs do not become excessive. Additionally, the type of computations performed are simplified to the level where Laplace's equations, rather than Poissons' equations are solved. That is, a particle charge in a given volume in space is assumed to not affect the potential at that location. All potentials in space are therefore defined by surface potentials only.

Figure 5 shows an overview of what NASCAP does. Once the spacecraft and its environment are defined, currents to each surface cell from the environment are defined if its potential is known:

$$I_{external}(V) = -I_{electron} + I_{ions} + I_{photo} + I_{secondaries} + I_{backscatter}$$

The internal currents flowing within the spacecraft are also defined if all of the surface potentials are known:

$$I_{internal} = (V_i - V_o)/R + C \frac{d}{dt} (V_i - V_o)$$

V_i = surface potential

V_o = structure potential (structure assumed to be conducting)

In this case the currents are functions of the difference between surface and structure potential. A consistent solution is obtained when the sum of all of the currents flowing to structure is zero:

Since all 812 surface cells are involved in this summation, an enormous number of computations are performed in each iteration.

As shown in the lower right-hand box in Figure 5, a Laplace's equation solution is obtained for each iteration of a set of surface potentials. This in itself is a very complicated (actually the most complex part) computation since so many surface cells and an even greater number of spatial volume cells must be included in the computation. The result of this side calculation is used to permit equipotential contours to be drawn in the space surrounding the spacecraft.

An even more important use for the Lacplace solution is to indicate situations in which a potential barrier exists at or off the surface of any given surface cell. Since photoelectrons and secondary emission electrons are emitted with only a few electron volts of energy, a potential barrier of a few volts effectively cuts off or prohibits any of these low energy electrons from leaving the surface. NASCAP, then, uses the Lacplace solution to cut off the emission of low energy electrons from any given surface cell as soon as a potential barrier is detected for that cell. The net result of this potential barrier effect can be an overwhelming change in the charging characteristics from what would be expected otherwise.

Environment

The synchronous orbit plasma environment used in the stress analysis uses a two-Maxwellian energy distribution for the electrons as well as the ions so that the differential flux for each species is given by

$$\frac{d\phi}{dE} = \frac{\phi_{01}}{(kT_1)^2} E\, e^{-\frac{E}{kT_1}} + \frac{\phi_{02}}{(kT_2)^2} E\, e^{-\frac{E}{kT_2}}$$

By selecting the two temperatures and two fluxes for each particle species the measured environment can be fitted very well. This is demonstrated in Figures 6 and 7. These curves have been generated from ATS-5 data as presented by Garrett.(2)

We see from these figures that whereas a single Maxwellian cannot be made to fit the data throughout the total energy range, the double Maxwellian fits nicely.

We therefore see that the static geosynchronous orbit environment can readily be described by specifying eight quantities:

a. Two electron temperatures
b. Two electron number densities

c. Two ion temperatures
d. Two ion number densities

Using these parameters, one can determine the fluxes.

The densities and temperatures were taken from Reference 1 with some modifications. In that study the plasma electron and ion densities, temperatures, and fluxes for a double-Maxwellian distribution were computed as a function of A_p and local time. In those computations the ATS plasma data were fitted to a model which made a linear adjustment of the parameters for the effects of magnetic activity. The flux of electrons and ions was enhanced with increasing A_p. In the stress analysis performed in the present study two different sets of environmental parameters were used, corresponding to different geomagnetic conditions. These are shown in Table 4.

A "worst" case environment corresponds to an A_p of 400 and a "severe" case corresponds to an A_p of 132. The fractional occurrence of A_p showing the percent occurrence of A_p from 1932-1975 is given in Figure 8. The A_p we have used differs from Garretts' by a factor of eight and is the commonly used daily average magnetic amplitude in units of 2 gamma, whereas the Garrett A_p is the sum of the trihourly A_p's and is not normally used in the literature. The densities and temperatures shown in Table 4 were selected to maximize the spacecraft chargeup under the selected conditions. The most severe chargeup does not necessarily occur when the flux of low energy electrons is maximized since these electrons produce secondaries which tend to decrease negative chargeup. Furthermore the large ion fluxes also limit chargeup. For these reasons those parameters which correspond to the largest high energy electron density but to the lowest low energy electron and ion densities were selected from the Garrett model for each A_p.

NASCAP Runs

Several NASCAP runs were performed to determine the location and the magnitude of environmentally induced voltage stresses. Not only were two different environments considered, but also for each environment three solar directions and an eclipse case were analyzed. The cases run are listed in Table 5. The worst case environment is identified by $A_p = 400$ and the severe environment by $A_p = 132$. The NASCAP code permits the direction of the sun relative to the spacecraft to be inserted. The sun can also be turned off to examine eclipse conditions. This was performed in Cases 4 and 8.

A special feature was added to NASCAP for use on this satellite. This feature permitted a spinning spacecraft with sun normal to the spin axis to be simulated by incorporating a spin averaged sun intensity into the program. This feature was used in Cases 3 and 7. The approach is valid since the charging times are long compared to the spacecraft spin period. Since NASCAP is a time dependent code it was necessary to run several cycles for each case, examine the resulting potentials and determine that steady state solution had been reached before changing conditions to the next case.

Results

The main outputs of the NASCAP program which were used for the stress analysis were the potentials on each of the 810 cells and the differences between each cell potential and the structure (conductor) potential. Tables 6 and 7 show a portion of the 810 cell potential and the conductor/cell potential difference printout. The samples shown are results from Case 7, $A_\rho = 400$, with the sun direction normal to the spin axis. These data along with a surface cell list, which identify the cells by material, location and orientation, permit one to determine the location and magnitude of the environmentally induced voltage stresses. Table 8 is a sample of the surface cell on the material plots, and the coordinates of the normal give its orientation. All the cells in the sample are identified as ceria doped coverglass on the solar paddles.

We have summarized the large volume of data detailing the potentials and stresses on the surface cells by extracting stresses greater than 1 kilovolt and identifying the materials and location of these large stresses for each of the cases run. When a group of contiguous cells of identical material was found having stresses larger than 1 kilovolt, the largest voltage stress of the group was recorded and located on the spacecraft. The results are shown in Figures 9 through 16. These data are the most significant result of the analysis. The stresses shown in the figures can be assumed to be axially symmetric for the same type of material. The structure potential for each case is also shown in the figures.

The largest potential differences between surface material and structure occur when the sun is normal to the spin axis and a larger fraction of the surface material has kilovolt stresses relative to the structure. For the $A_\rho = 132$ (severe) environment (Figure 11) the potential difference can be as large as 1900 volts. This can occur on the upper teflon portions of the sun shade. In the worst case environment the teflon on the shade can have a potential difference as high as 3720 volts relative to structure. This potential difference is much lower than one would obtain if the "barrier" effect were not included in NASCAP. The low stress predicted by NASCAP in this worst case environment is surprising in view of the numerous reports of arc effects on synchronous orbit spacecraft. Even though the stresses are most severe during side sun conditions, stresses greater than 1 kilovolt are found for all the cases considered. Therefore all the materials and locations identified in Figures 9 through 16 can be the source of an electrostatic discharge if discharges occur at 1 kilovolt.

Another interesting set of outputs generated by NASCAP is the potential contour plots around the spacecraft. Several such plots are made for each case considered. A few samples of the contour plots are shown in Figures 17 through 19 for the worst case environment with the spacecraft in eclipse, sun at -Z and side sun. The contour lines inside the spacecraft are artifacts of the program and should be considered to close along the surface.

The labels Z_{min}, Z_{max} and ΔZ on the figures represent the minimum potential contour voltage, the maximum voltage and the voltage between contours. These types of plots can be used to quickly determine the regions

of high potential on the spacecraft, the innermost contours being the largest negative potential (i.e., Z_{min}). In Figure 17, in the sun -Z case, notice that the regions of highest potential are on the lower portion of the sun shade, the second surfaced mirror area below the shade and the mirrored area above the conical array. On the other hand, the regions of large potential are not regions of large voltage stress as indicated by the smoothness of the contour and its relationship to the spacecraft surface contour. In this case, the largest stresses occur on the solar paddles near Z = -5. Both Figures 17 and 18 show contours that do not indicate large surface potential changes. In contrast to these, Figure 19, which shows the distortion in the equipotential contours for the side sun case, is indicative of large voltage stresses on the surface.

Conclusions and Recommendations

The application of NASCAP to a specific satellite to determine its charging characteristics is a reasonably straightforward process for personnel familiar with computer languages and with the field of spacecraft charging. The capabilities associated with NASCAP are continually being upgraded. A few improvements of NASCAP that are suggested have to do with the accessibility of the computational results such as the identification of high stress locations in either tabular or graphical form. The high stress threshold should be entered as a part of the material characterization. One other additional feature which would be useful would be the direct computation of the steady state potentials by elimination of element capacitances. This would circumvent the repetition of runs to examine whether the steady state had been reached.

In regard to the accuracy of NASCAP itself, a few laboratory experiments have been performed[3] which verify predictions on small sample measurements. A NASCAP charging analysis of the SCATHA satellite has been performed,[4] but correlative data between in-flight performance and the analysis predictions have not yet been published. As noted in the section on the voltage stress analysis results, the very worst case stress of 3720 volts is unexpectedly low as compared to previous stress computations in which the potential barrier effect was not taken into account. In view of laboratory measurements[5] which indicate much higher voltage breakdown thresholds (usually 8 kV to 12 kV), one wonders whether the barrier effect is overemphasized in NASCAP, or if some other mechanism must be postulated to account for the numerous reports of in-orbit anomalies due to spacecraft charging. On the other hand, there are many other possible explanations for the apparent discrepancy. For example,

- Laboratory tests may not reflect true space flight configurations.
- The observed anomalies in orbit are caused by arcing resulting from differential stresses less than 4 kilovolts.
- The material properties, e.g., secondary and photoemission, may not be adequately known for the high stress and real in-orbit environment to permit accurate charging/discharging computations.
- The modeling of the spacecraft for NASCAP may be too coarse to permit the accurate computation of stresses at edges and sharp points.

REFERENCES

References 1 through 4 were papers presented at the USAF/NASA Spacecraft Charging Technology Conference, 31 Oct. to 2 Nov. 1978, U.S. Air Force Academy, Colorado:

1. I, Katz, J. J. Cassidy, M. J. Mandell, G. W. Schnuelle, P. G. Steen, and J. C. Roche, "The Capabilities of the NASA Charging Analyzer Program."
2. H. B. Garrett, "Modeling of the Geosynchronous Plasma Environment."
3. J. C. Roche and C. K. Purvis, "Comparison of NASCAP Predictions with Experimental Data."
4. D. E. Parks, I. Katz, G. W. Schnuelle, M. J. Mandell, and A. Rubin, "Charging Analysis of the SCATHA Satellite."
5. N. J. Stevens, F. D. Berkopec, J. V. Staskus, R. A. Bleck, and S. J. Narcisco, "Testing of Typical Spacecraft Materials in a Simulated Substorm Environment," Proceedings of the Spacecraft Charging Technology Conference, AFGL-TR-77-0051, NASA TM X-73537, 24 Feb. 1977.

ACKNOWLEDGEMENTS

The work reported here was sponsored by the Air Force. The cooperation of the S^3 staff, particularly J. Cassidy and I. Katz, was immensely helpful in getting us started and in working out problems. Mrs. B. Benefield's typing and assembling of the manuscript and figures is gratefully acknowledged.

Table 1. Material Properties for Exposed Surfaces

Property[b]	GOLD	SOLAR	WHITEN	SCREEN	BLACKC YELOWC	GOLDPD	KAPTON
1	-	4.00+00	3.50+00	-	3.50+00	-	3.50+00
2	1.00-03	1.79-04	5.00-05	1.00-03	5.00-05	1.00-03	1.25-04
3	∞	1.00-14	5.90-14	∞	5.00-10	∞	1.00-14
4	7.90+01	1.00+01	5.00+00	1.00+00	5.00+00	7.01+01	5.00+00
5	8.80-01	4.10+00	2.10+00	0.00	2.10+00	1.03+00	2.10+00
6	8.00-01	4.10-01	1.50-01	1.00+00	1.50-01	7.20-01	1.50-01
7	8.30+01	-1.00+00	-1.00+00	1.00+01	-1.00+00	8.30+01	-1.00+00
8	1.63+00	0.00	0.00	1.50+00	0.00	1.63+00	0.00
9	3.46+01	2.30+00	1.05+00	0.00	1.05+00	3.46+01	1.42+00
10	7.00-01	2.08+01	9.80+00	1.00+00	9.80+00	7.00-01	9.80+00
11	4.00-01	1.36+00	1.40+00	0.00	1.40+00	4.00-01	1.40+00
12	5.00+01	4.00+01	7.00+01	1.00+00	7.00+01	5.00+01	7.00+01
13	2.90-05	2.00-05	2.00-05	0.00	2.00-05	2.90-05	2.00-05

	SIO2	TEFLON	INDOX	YGOLDC	ALUMIN	BOOMAT[c]	ML12
1	4.00+00	2.00+00	-	-	-	2.00+00	-
2	2.75-04	1.25-04	1.00-03	1.00-03	1.00-03	5.00-03	1.00-03
3	2.75-12	1.00-14	∞	∞	∞	1.00-10	∞
4	1.00+01	1.00+01	2.44+01	4.20+01	1.30+01	6.34+01	6.00+00
5	2.40+00	3.00+00	1.40+00	1.49+00	9.70-01	1.86+00	1.00+00
6	4.00-01	3.00-01	8.00-01	4.80-01	3.00-01	5.90-01	3.00-01
7	-1.00+00	-1.00+00	-1.00+00	-1.00+00	2.60+02	8.30+01	-1.00+00
8	0.00	0.00	0.00	0.00	1.30+00	1.63+00	0.00
9	1.02+00	2.00+00	7.18+00	1.02+01	2.40+02	3.46+01	2.00+00
10	2.00+01	1.67+01	5.55+01	4.20+01	1.73+00	7.00-01	1.20+01
11	1.40+00	1.40+00	1.36+00	1.00+00	1.36+00	4.00-01	1.40+00
12	7.00+01	7.00+01	4.00+01	6.00+01	4.00+01	5.00+01	7.00+01
13	2.00-05	2.00-05	3.20-05	2.40-05	4.00-05	2.72-05	2.10-05

Table 2. Material Properties Descriptions

Property 1:	Relative dielectric constant for insulators (dimensionless).
Property 2:	Thickness of dielectric film or vacuum gap (meters).
Property 3:	Electrical conductivity (mho/m). The value = indicates a vacuum gap over a conducting surface.
Property 4:	Atomic number (dimensionless).
Property 5:	Maximum secondary electron yield for electron impact at normal incidence (dimensionless).
Property 6:	Primary electron energy to produce maximum yield at normal incidence (keV).
Property 7-10:	Range for incident electrons. Either: $\text{Range} = P_7 E^{P_8} + P_9 E^{P_{10}}$ where the range is in angstroms and for the energy in keV or $P_7 = -1.$ to indicate use of an empirical range formula $P_9 = \text{density } (g/cm^3)$ $P_{10} = \text{mean atomic weight (dimensionless).}$
Property 11:	Secondary electron yield for normally incident 1 keV protons.
Property 12:	Proton energy to produce maximum secondary electron yield (keV).
Property 13:	Photoelectron yield for normally incident sunlight (A/m2).

Table 3. Satellite Charging Model Materials List

Name	Material Description	Spacecraft Locations	Thickness and Conductivity
1. SSM (SIO2)	10 mil SIO2 (Fused Quartz)	Second Surface Mirrors (SSMs)	10 mils = 254 μm, 10^{-16} mho/m
2. SSM (SIO2)	8 mil SIO2 (Fused Quartz)	SSMs	8 mils = 200 μm, 10^{-16} mho/m
3. Ceria (SIO2)	6 mil Ceria Glass (may become quartz)	Paddle Solar Cell Covers	6 mils = 150 μm, 10^{-16} mho/m
4. Micro (SIO2)	6 mil Microsheet Borosilicate Glass	Cylindrical and Conical Solar Cells Cover-glasses	6 mils = 150 μm, 10^{-16} mho/m
5. Whiten	White Paint	Collar Top Bottom of Spacecraft	2 mils = 50 μm, 5.10^{-12} mho/m
6. Black C	Black Paint	Top and Parts of Paddle	2 mils = 50 μm, 5.10^{-10} mho/m
7. Teflon	Teflon Thermal Blankets	Sunshade Top of RADECs	2 mils = 50 μm, 10^{-16} mho/m
8. Aluminum	Aluminum	Structural Parts	---

Table 4. Plasma Parameters used in NASCAP Runs

Case 1. A_p = 400 (Worst Case)				
	Low E Maxwellian		High E Maxwellian	
	$N_1(cc^{-1})$	$T_1(eV)$	$N_2(cc^{-1})$	$T_2(eV)$
Electrons	7.6	222	5.7	13,300
Ions	1.6	140	1.8	7,300
Case 2. A_p = 132 (Severe)				
Electrons	2.5	234	1.66	11,300
Ions	1.0	270	0.85	10,800

Table 5. Cases Run on NASCAP

Case No.	A_p	Sun Direction*
1	132	+Z
2	132	-Z
3	132	$\perp$Z (Spin)
4	132	(Eclipse)
5	400	+Z
6	400	-Z
7	400	$\perp$Z (Spin)
8	400	(Eclipse)

*+Z is parallel to spin axis, toward sensor.

Table 6. Sample of Surface Potentials (Volts) of the 810 Cells

SURFACE POTENTIALS - ALL 810 CELLS

CELL NO.						CELL NO.
1	-1.0148+04	-1.0148+04	-1.0148+04	-1.0148+04	-1.0148+04	5
6	-1.0148+04	-1.0148+04	-1.0148+04	-1.0148+04	-1.0148+04	10
11	-1.0148+04	-1.0148+04	-1.0148+04	-1.0148+04	-1.0148+04	15
16	-1.0148+04	-1.0148+04	-1.0148+04	-1.0148+04	-1.0148+04	20
21	-1.0148+04	-1.0148+04	-1.0148+04	-1.0148+04	-1.0148+04	25
26	-1.0148+04	-1.0148+04	-1.0148+04	-1.0148+04	-1.0148+04	30
31	-9.0054+03	-8.9576+03	-1.0148+04	-1.0148+04	-9.0513+03	35
36	-9.0497+03	-1.0148+04	-1.0148+04	-1.0089+04	-1.0006+04	40
41	-9.0763+03	-9.0763+03	-8.9352+03	-9.0657+03	-1.0148+04	45
46	-1.0148+04	-8.9503+03	-9.0823+03	-1.0148+04	-1.0148+04	50
51	-8.9118+03	-8.8851+03	-1.0148+04	-1.0148+04	-8.8599+03	55
56	-8.7239+03	-9.4344+03	-8.3359+03	-9.5613+03	-8.5494+03	60
61	-9.0912+03	-7.8520+03	-7.1847+03	-6.7725+03	-6.1758+03	65
66	-6.0580+03	-6.0114+03	-5.9698+03	-5.9927+03	-9.5088+03	70
71	-8.5652+03	-9.0912+03	-7.7536+03	-7.0789+03	-6.5658+03	75
76	-6.2332+03	-6.1118+03	-6.1374+03	-9.0763+03	-6.0066+03	80
81	-9.4398+03	-8.5465+03	-9.0912+03	-7.7424+03	-7.0697+03	85
86	-6.5675+03	-6.2455+03	-6.1513+03	-6.2121+03	-9.0763+03	90
91	-6.5066+03	-6.1981+03	-9.4897+03	-6.2727+03	-6.0529+03	95
96	-9.4994+03	-8.5380+03	-9.0912+03	-7.7243+03	-7.0594+03	100
101	-6.5592+03	-6.2316+03	-6.1111+03	-6.1382+03	-9.0763+03	105
106	-6.0454+03	-6.1138+03	-9.4896+03	-6.0694+03	-6.0018+03	110
111	-9.5447+03	-8.5030+03	-9.0912+03	-7.9126+03	-7.1449+03	115
116	-6.6363+03	-6.2309+03	-6.1465+03	-5.9705+03	-5.9998+03	120
121	-6.0530+03	-9.4149+03	-8.2879+03	-1.0148+04	-1.0148+04	125
126	-1.0148+04	-1.0148+04	-1.0148+04	-1.0148+04	-8.8600+03	130
131	-8.7319+03	-9.4154+03	-8.2915+03	-9.0912+03	-7.7681+03	135
136	-7.4694+03	-6.7305+03	-6.2051+03	-6.1228+03	-5.9569+03	140
141	-5.8423+03	-5.8327+03	-9.0912+03	-5.7910+03	-5.9936+03	145
146	-9.1222+03	-6.8382+03	-9.0932+03	-9.4900+03	-6.3115+03	150
151	-9.1074+03	-9.4900+03	-6.2141+03	-9.0912+03	-5.7692+03	155
156	-6.4738+03	-9.0912+03	-7.7817+03	-7.5047+03	-6.7580+03	160
161	-6.2304+03	-6.0243+03	-5.9289+03	-6.0102+03	-5.9930+03	165
166	-9.4396+03	-8.3471+03	-1.0148+04	-1.0148+04	-9.0054+03	170
171	-8.9578+03	-1.0148+04	-1.0148+04	-1.0148+04	-1.0148+04	175
176	-1.0148+04	-1.0148+04	-1.0148+04	-1.0148+04	-1.0148+04	180
181	-1.0148+04	-8.9292+03	-8.9114+03	-9.5458+03	-8.5065+03	185
186	-9.0912+03	-7.8977+03	-7.1360+03	-6.7072+03	-6.1981+03	190
191	-6.0824+03	-5.9676+03	-5.9752+03	-5.9812+03	-9.0912+03	195
196	-6.0292+03	-5.9945+03	-1.0148+04	-6.2765+03	-6.1019+03	200
201	-5.5923+03	-5.8345+03	-5.2433+03	-5.5727+03	-9.0912+03	205
206	-5.5905+03	-1.0148+04	-6.6947+03	-6.0580+03	-5.6467+03	210
211	-5.4388+03	-5.4568+03	-9.0912+03	-5.5363+03	-1.0148+04	215
216	-7.6603+03	-6.2620+03	-5.7271+03	-5.4801+03	-5.4983+03	220
221	-9.0912+03	-5.5995+03	-1.0148+04	-7.6325+03	-6.2422+03	225
226	-5.7217+03	-5.4742+03	-5.4757+03	-9.0912+03	-5.5452+03	230
231	-1.0148+04	-6.3253+03	-6.4560+03	-5.8424+03	-5.9328+03	235

Table 7. Sample of Potential Differences (Volts) of the 810 Cells

CONDUCTOR 1 POTENTIAL = -9.0763+03

POTENTIAL DIFFERENCES - ALL 810 CELLS

CELL NO.						CELL NO.
1	-1.0713+03	-1.0713+03	-1.0713+03	-1.0713+03	-1.0713+03	5
6	-1.0713+03	-1.0713+03	-1.0713+03	-1.0713+03	-1.0713+03	10
11	-1.0713+03	-1.0713+03	-1.0713+03	-1.0713+03	-1.0713+03	15
16	-1.0713+03	-1.0713+03	-1.0713+03	-1.0713+03	-1.0713+03	20
21	-1.0713+03	-1.0713+03	-1.0713+03	-1.0713+03	-1.0713+03	25
26	-1.0713+03	-1.0713+03	-1.0713+03	-1.0714+03	-1.0713+03	30
31	7.0922+01	1.1865+02	-1.0714+03	-1.0713+03	2.4974+01	35
36	2.6528+01	-1.0714+03	-1.0713+03	-1.0127+03	-9.2980+02	40
41	0.0000	0.0000	1.4104+02	1.0538+01	-1.0714+03	45
46	-1.0713+03	1.2599+02	-5.9917+00	-1.0714+03	-1.0713+03	50
51	1.6450+02	1.9121+02	-1.0714+03	-1.0713+03	2.1641+02	55
56	3.5239+02	-3.5815+02	7.4038+02	-4.8504+02	5.2689+02	60
61	-1.4916+01	1.2243+03	1.8916+03	2.3038+03	2.9005+03	65
66	3.0183+03	3.0649+03	3.1065+03	3.0835+03	-4.3252+02	70
71	5.1105+02	-1.4916+01	1.3227+03	1.9974+03	2.5105+03	75
76	2.8431+03	2.9645+03	2.9389+03	0.0000	3.0697+03	80
81	-3.6354+02	5.2979+02	-1.4916+01	1.3339+03	2.0066+03	85
86	2.5088+03	2.8307+03	2.9249+03	2.8641+03	0.0000	90
91	2.5697+03	2.8782+03	-4.1341+02	2.8036+03	3.0233+03	95
96	-4.2309+02	5.3826+02	-1.4916+01	1.3520+03	2.0169+03	100
101	2.5171+03	2.8447+03	2.9652+03	2.9381+03	0.0000	105
106	3.0309+03	2.9625+03	-4.1335+02	3.0069+03	3.0744+03	110
111	-4.6846+02	5.7332+02	-1.4916+01	1.1636+03	1.9313+03	115
116	2.4399+03	2.8453+03	2.9298+03	3.1058+03	3.0765+03	120
121	3.0233+03	-3.3858+02	7.6842+02	-1.0713+03	-1.0713+03	125
126	-1.0713+03	-1.0713+03	-1.0714+03	-1.0713+03	2.1633+02	130
131	3.4443+02	-3.3912+02	7.8473+02	-1.4916+01	1.3081+03	135
136	1.6069+03	2.3458+03	2.8712+03	2.9535+03	3.1193+03	140
141	3.2340+03	3.2436+03	-1.4916+01	3.2853+03	3.0827+03	145
146	-4.5953+01	2.2381+03	-1.6921+01	-4.1377+02	2.7648+03	150
151	-3.1096+01	-4.1377+02	2.8622+03	-1.4912+01	3.3071+03	155
156	2.6024+03	-1.4916+01	1.2946+03	1.5716+03	2.3183+03	160
161	2.8459+03	3.0519+03	3.1473+03	3.0661+03	3.0833+03	165
166	-3.6333+02	7.2918+02	-1.0714+03	-1.0713+03	7.0922+01	170
171	1.1846+02	-1.0713+03	-1.0713+03	-1.0713+03	-1.0713+03	175
176	-1.0713+03	-1.0713+03	-1.0713+03	-1.0713+03	-1.0714+03	180
181	-1.0713+03	1.4706+02	1.6483+02	-4.6948+02	5.6978+02	185
186	-1.4916+01	1.1785+03	1.9403+03	2.3691+03	2.8762+03	190
191	2.9939+03	3.1086+03	3.1011+03	3.0951+03	1.4912+01	195

Table 8. Sample of Surface Cell List

SURFACE CELL LIST CELL NO.	CODE	CONDUCTOR	IX	IY	IZ	NORMAL	MATERIAL
1	0103060301O3	1	2	6	3	0 0 1	CERIA
2	0103060403O3	1	2	6	4	0 0 -1	CERIA
3	0103070301O3	1	2	7	3	0 0 1	CERIA
4	0103070403O3	1	2	7	4	0 0 -1	CERIA
5	0103080301O3	1	2	8	3	0 0 1	CERIA
6	0103080403O3	1	2	8	4	0 0 -1	CERIA
7	0103090301O3	1	2	9	3	0 0 1	CERIA
8	0103090403O3	1	2	9	4	0 0 -1	CERIA
9	0103100301O3	1	2	10	3	0 0 1	CERIA
10	0103100403O3	1	2	10	4	0 0 -1	CERIA
11	0103110301O3	1	2	11	3	0 0 1	CERIA
12	0103110403O3	1	2	11	4	0 0 -1	CERIA
13	0103120301O3	1	2	12	3	0 0 1	CERIA
14	0103120403O3	1	2	12	4	0 0 -1	CERIA
15	0103060301O3	1	3	6	3	0 0 1	CERIA
16	0103060403O3	1	3	6	4	0 0 -1	CERIA
17	0103070301O3	1	3	7	3	0 0 1	CERIA
18	0103070403O3	1	3	7	4	0 0 -1	CERIA
19	0103080301O3	1	3	8	3	0 0 1	CERIA
20	0103080403O3	1	3	8	4	0 0 -1	CERIA
21	0103090301O3	1	3	9	3	0 0 1	CERIA
22	0103090403O3	1	3	9	4	0 0 -1	CERIA
23	0103100301O3	1	3	10	3	0 0 1	CERIA
24	0103100403O3	1	3	10	4	0 0 -1	CERIA
25	0103110301O3	1	3	11	3	0 0 1	CERIA
26	0103110403O3	1	3	11	4	0 0 -1	CERIA
27	0103120301O3	1	3	12	3	0 0 1	CERIA
28	0103120403O3	1	3	12	4	0 0 -1	CERIA
29	0104060301O3	1	4	6	3	0 0 1	CERIA
30	0104060403O3	1	4	6	4	0 0 -1	CERIA

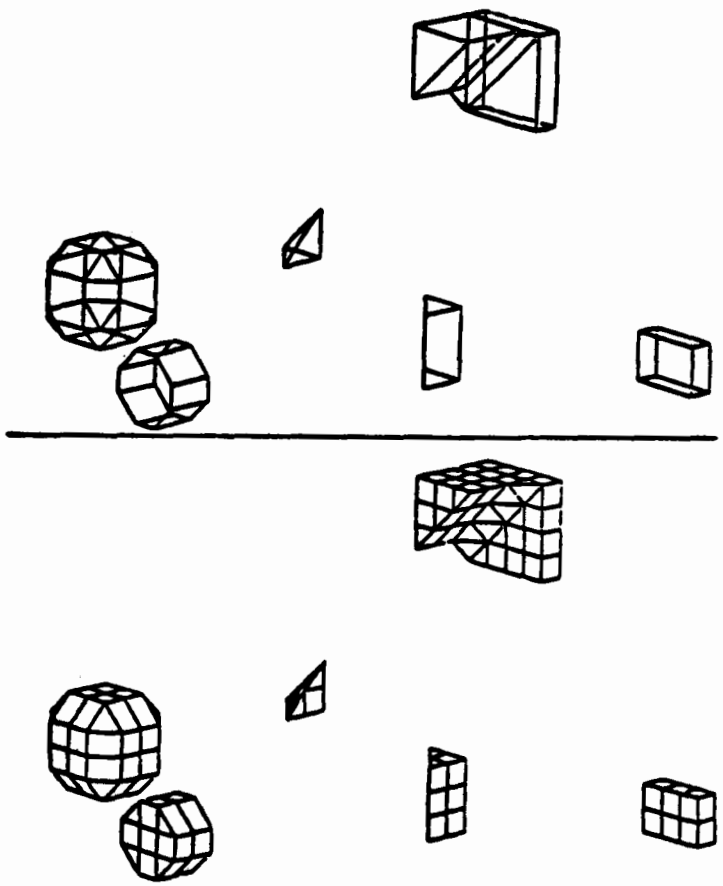

Figure 1. The six building block types are shown here. The uppermost object shows a FIL111 smoothing a corner. Below, from left to right are quasisphere, octagon right cylinder, tetrahedron, wedge, and rectangular parallelepiped.

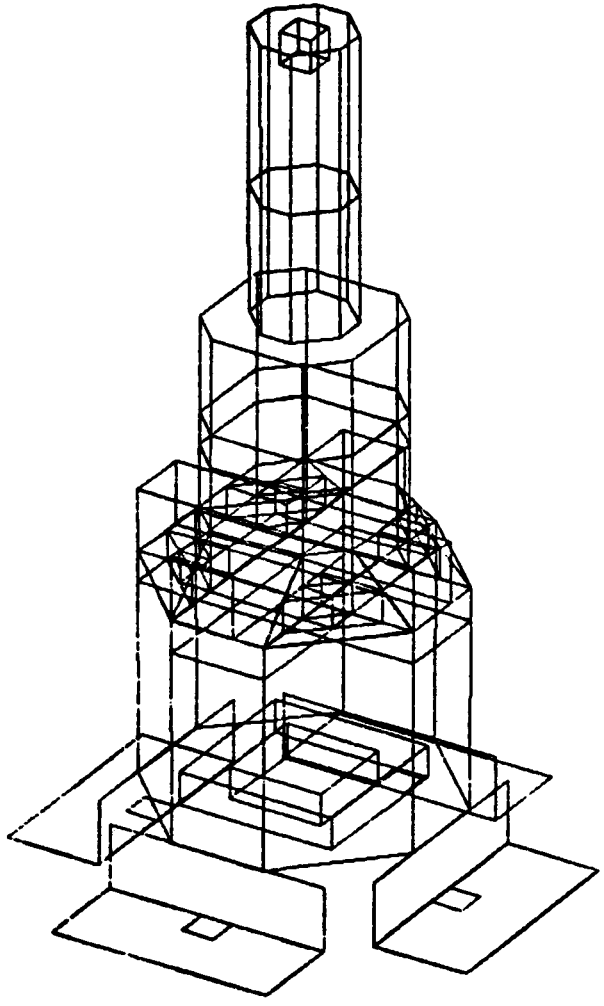

Figure 2. Building blocks used to define the satellite.

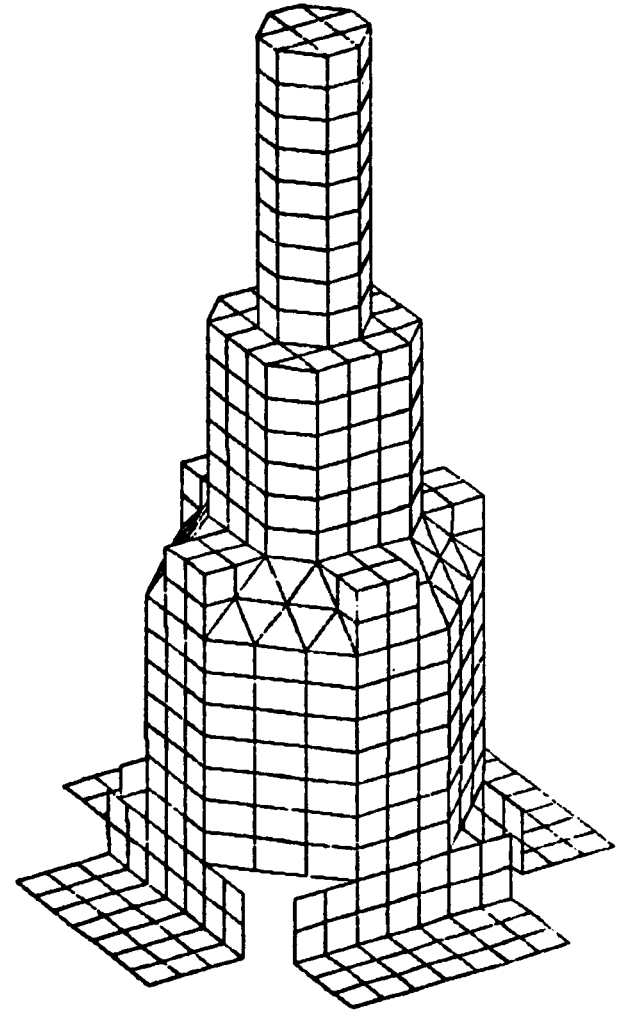

Figure 3. NASCAP drawing of the satellite showing surface cells.

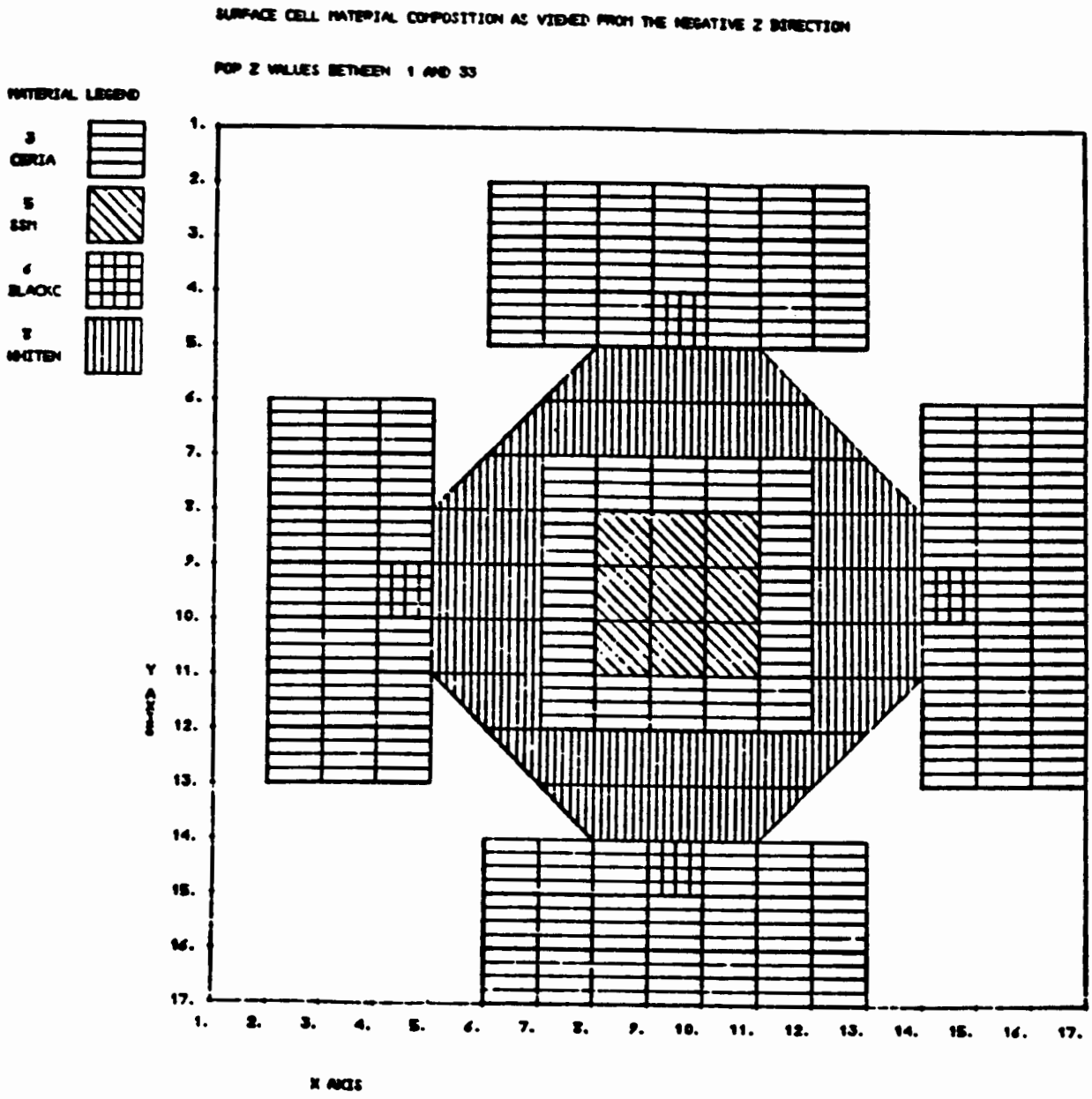

Figure 4. Surface cell material composition as viewed from the negative Z direction for Z values between 1 and 33.

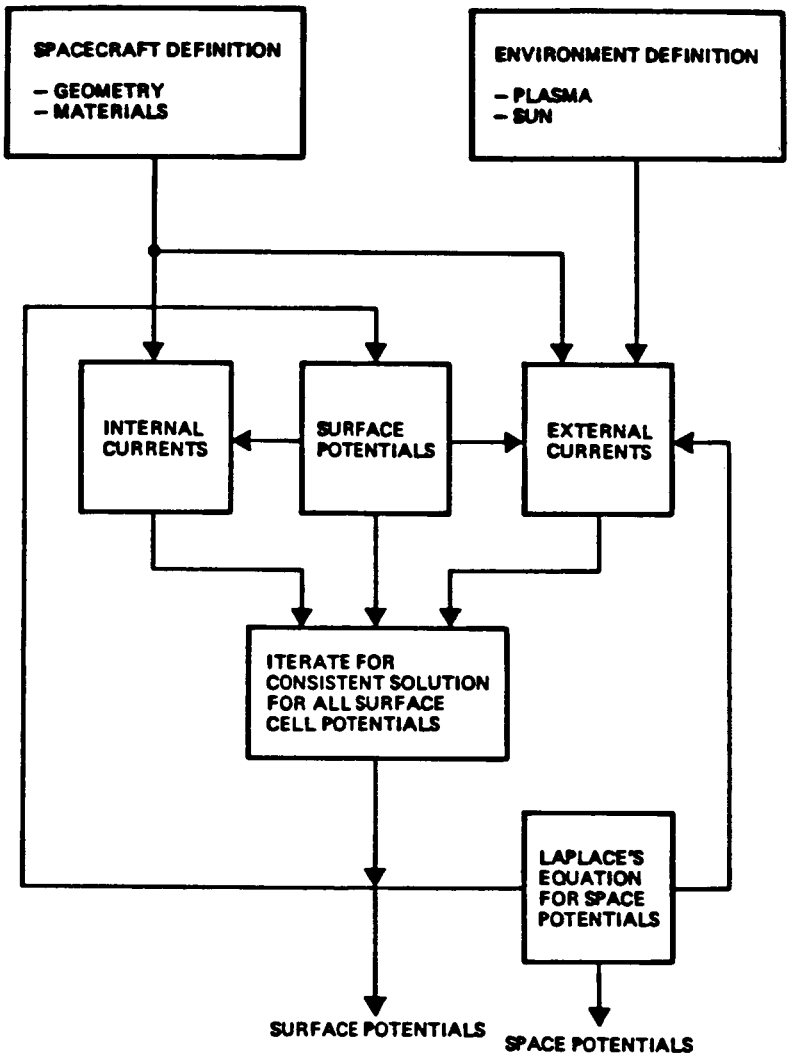

Figure 5. Overview of the NASCAP code.

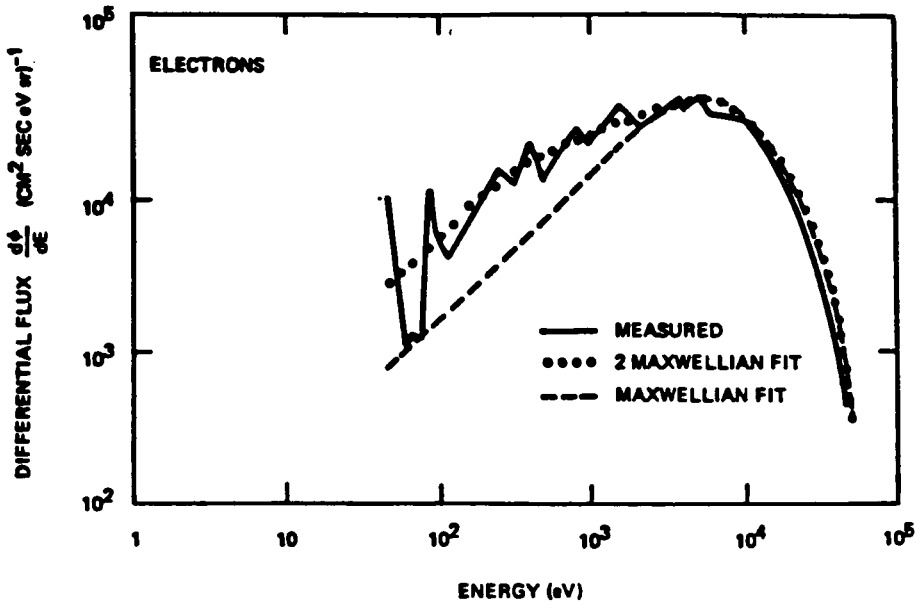

Figure 6. Differential flux of electrons (Sept. 30, 1969, ATS-5).

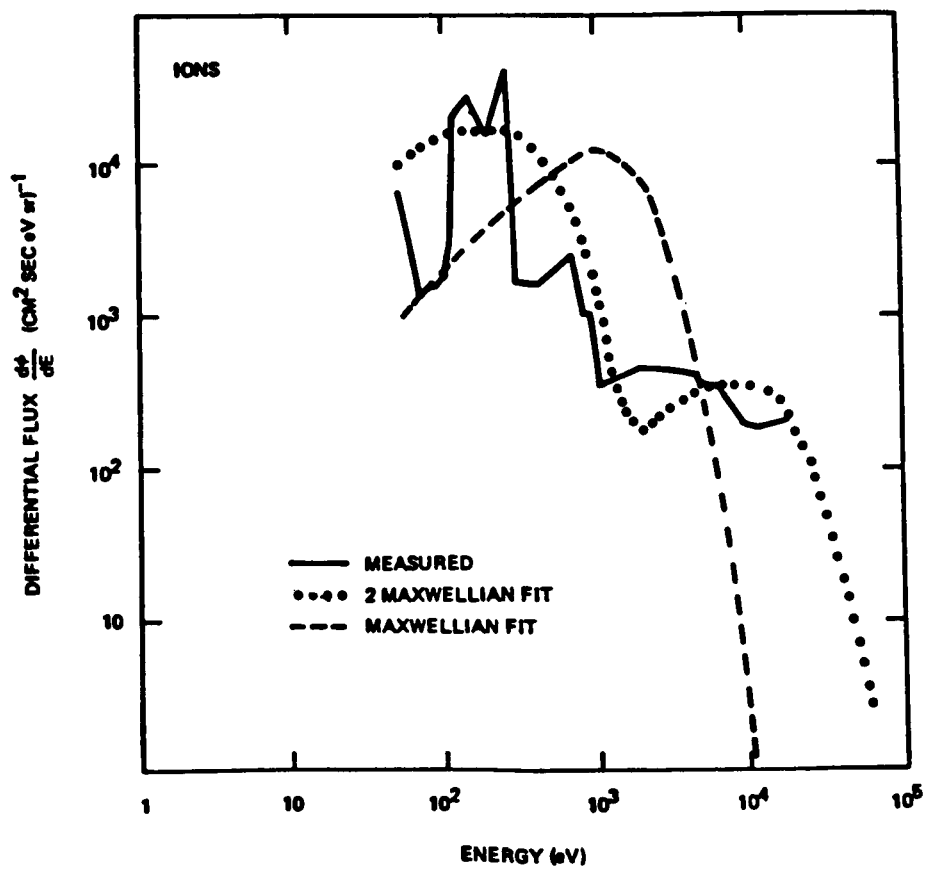

Figure 7. Differential flux of ions (Sept. 30, 1969, ATS-6).

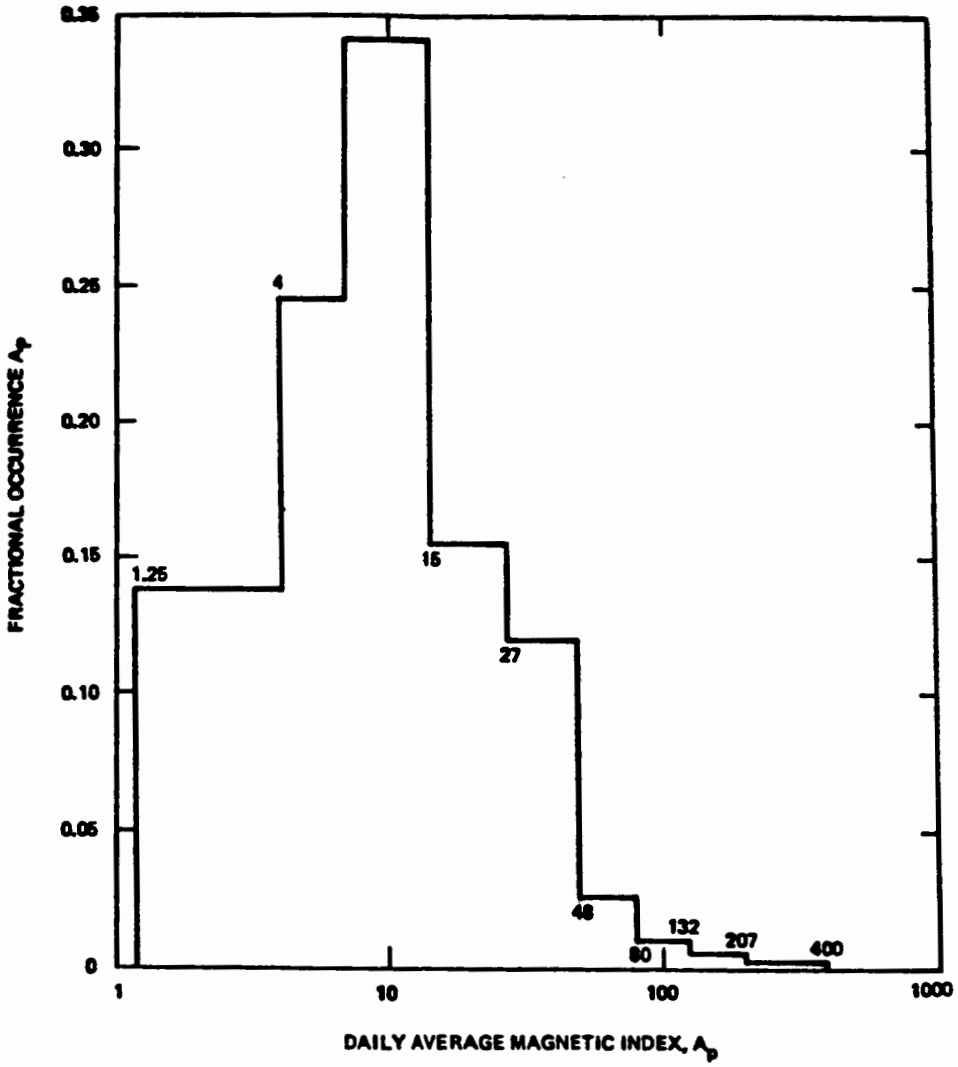

Figure 8. Occurrence of A_p from 1932-1975.

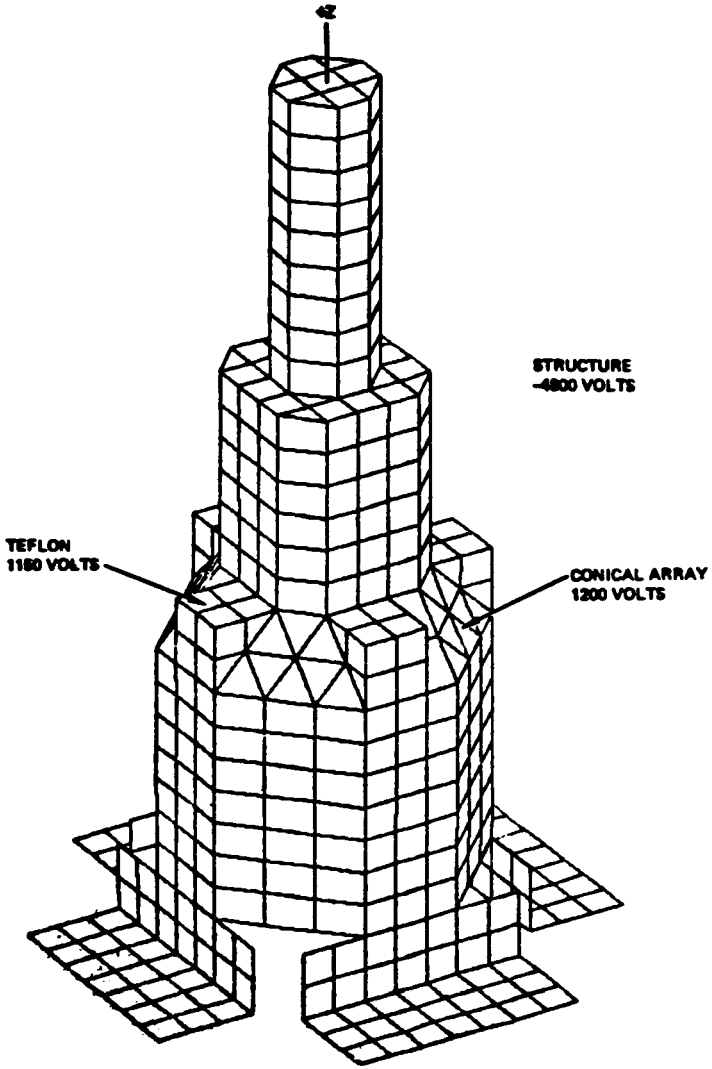

Figure 9. Case 1 - Maximum differential stress (sun +Z) ($\Delta V > 1000$ V) $A_p = 132$.

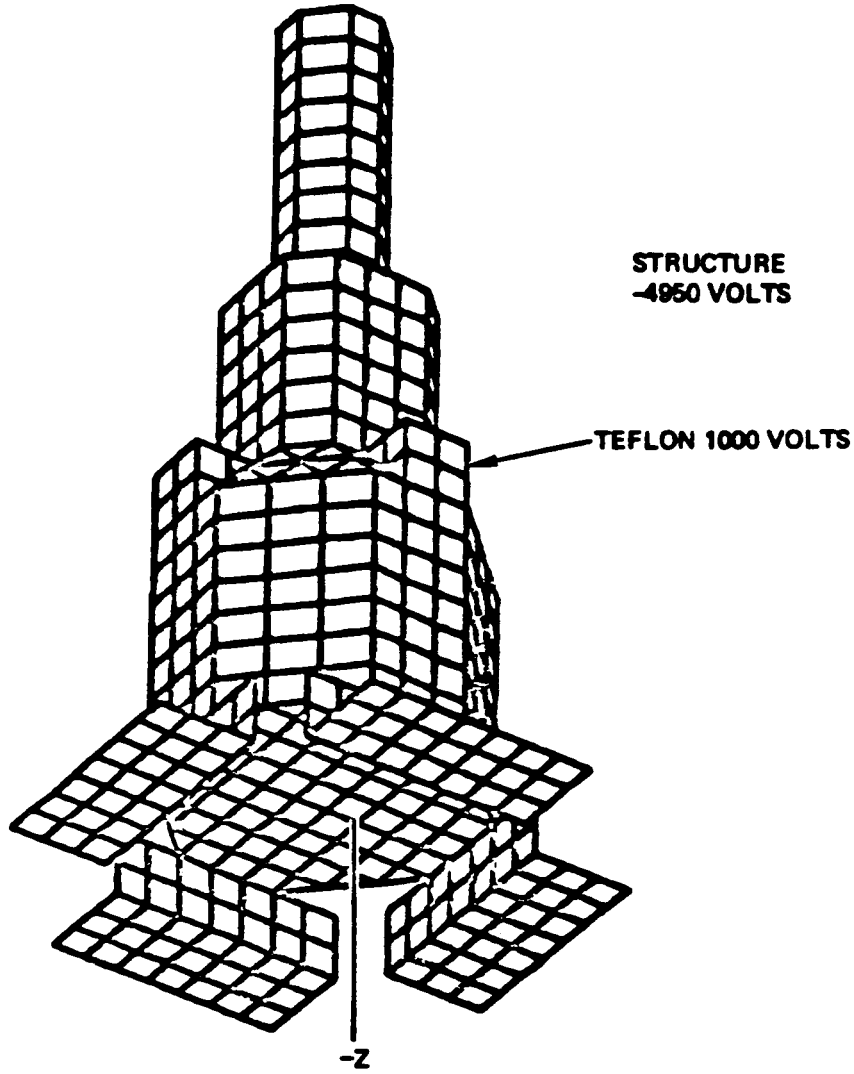

Figure 10. Case 2 - Maximum differential stress (sun -Z) ($\Delta V > 1000$ V) $A_p = 132$.

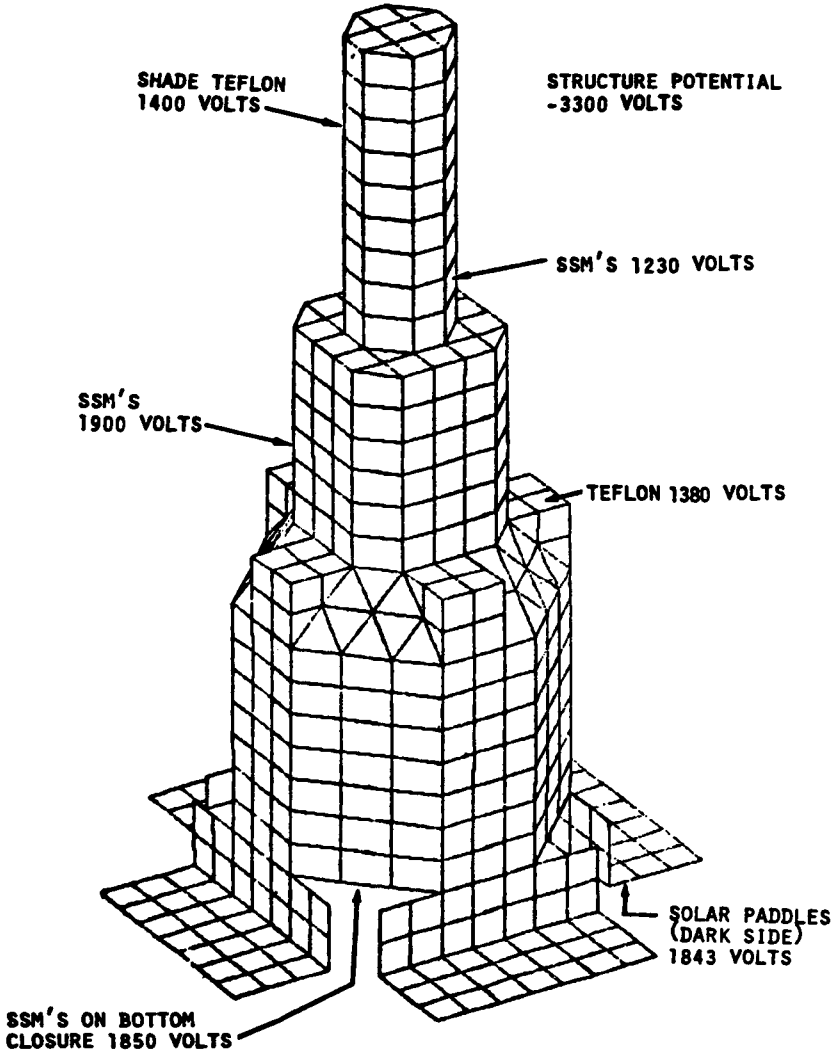

Figure 11. Case 3 - Differential stress (sun $\perp Z$, spin, A_p = 132) ($\Delta V > 1000$ V).

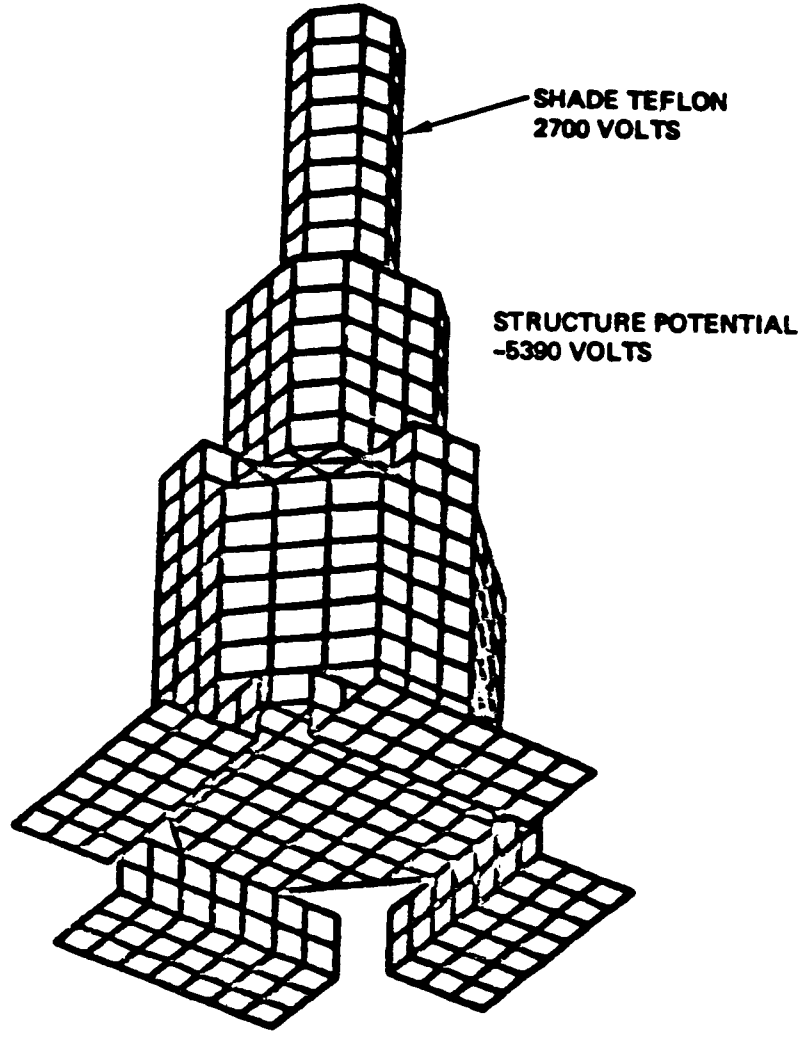

Figure 12. Case 4 - Differential stress (eclipse, A_p = 132)($\Delta V > 1000$ V).

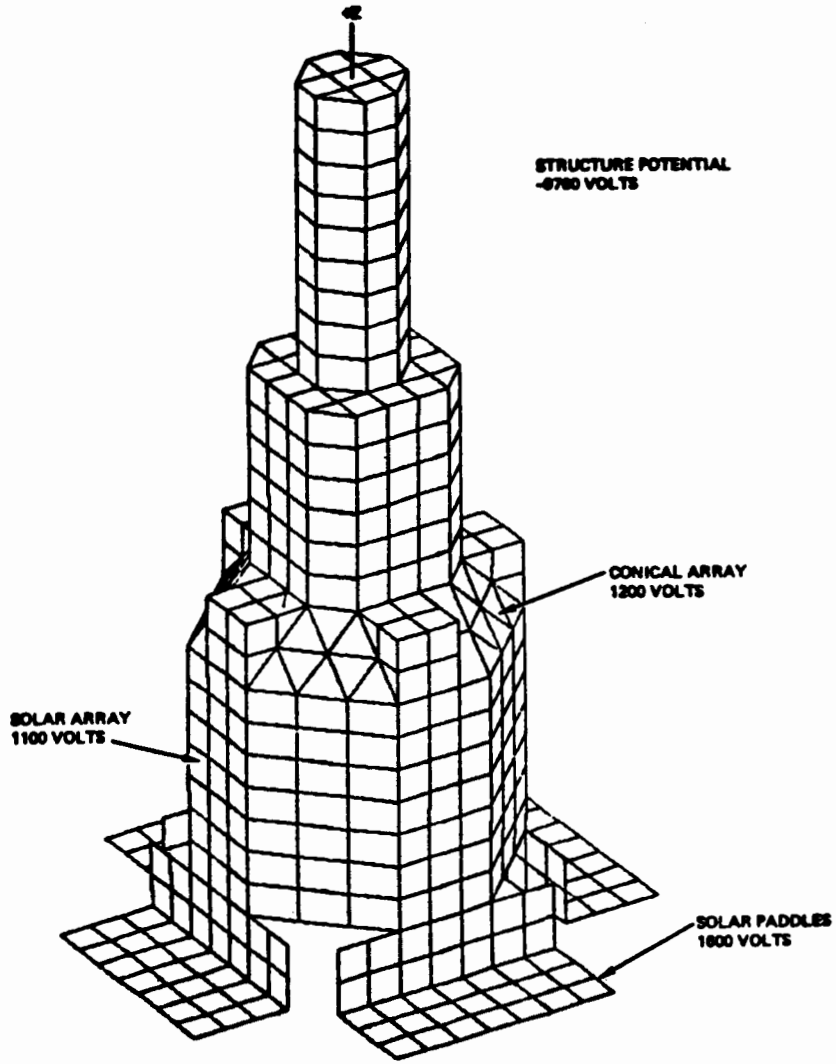

Figure 13. Case 5 - Differential stress (sun +Z, A_p = 400) ($\Delta V > 1000$ V).

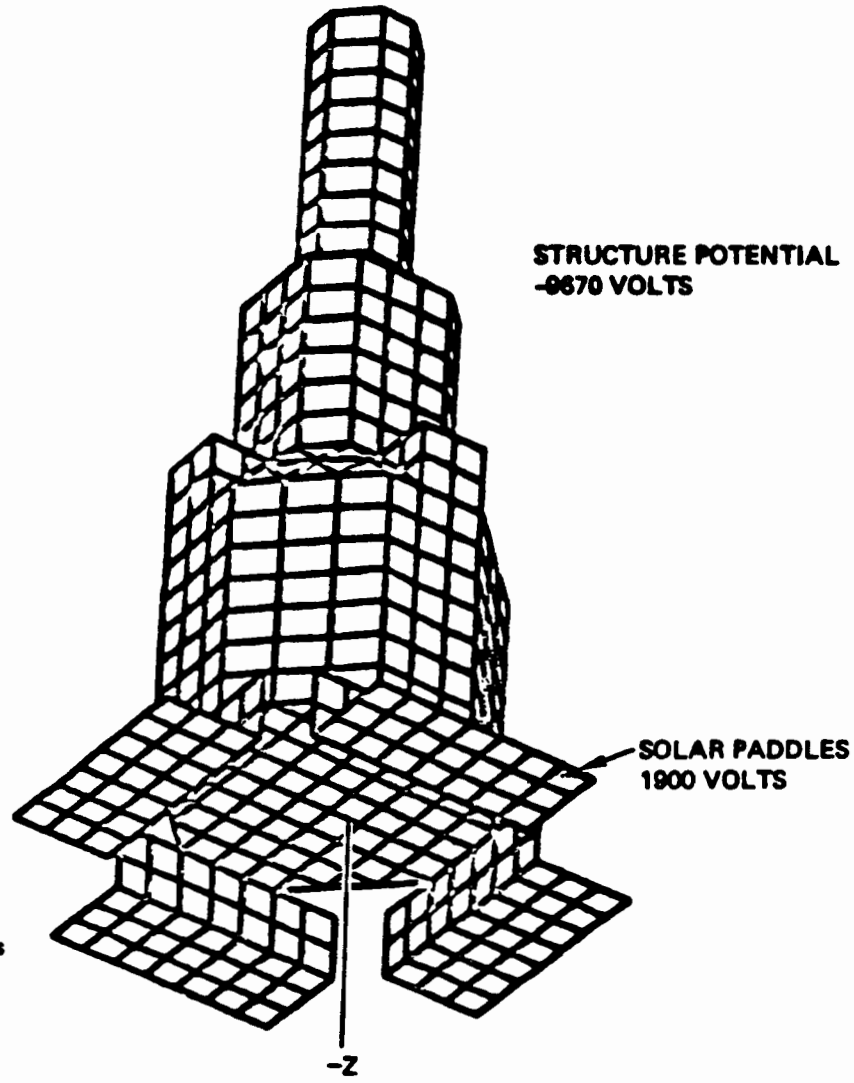

Figure 14. Case 6 - Differential stress (sun -Z, A_p = 400) ($\Delta V > 1000$ V).

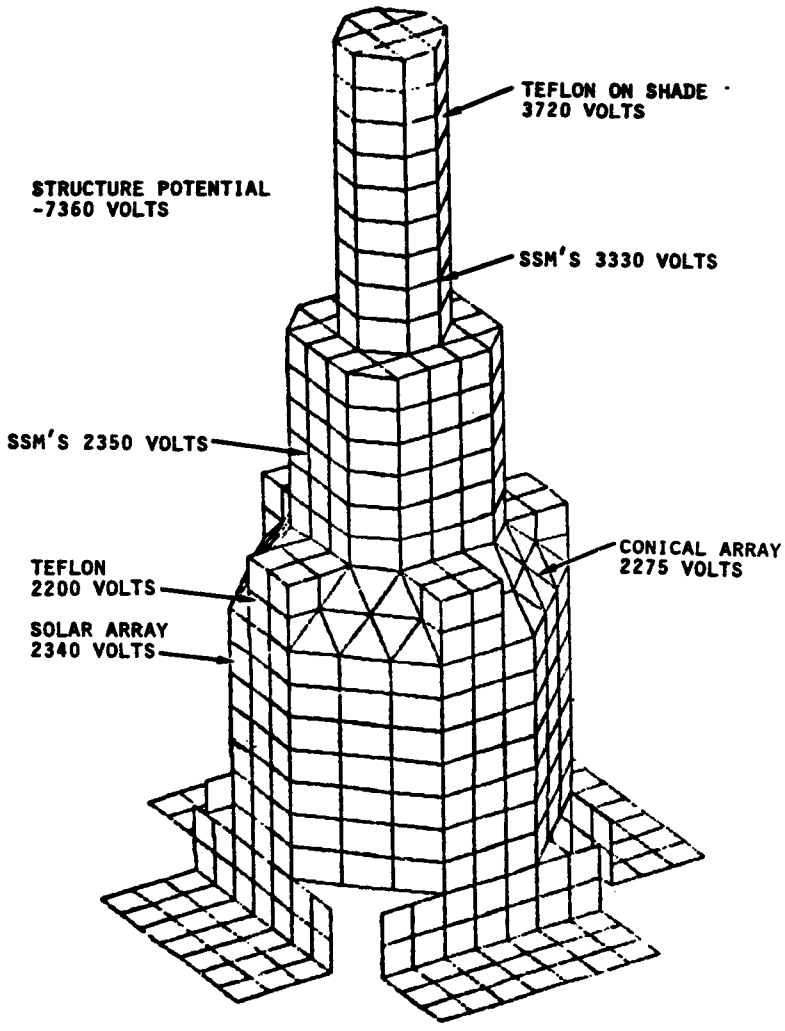

Figure 15. Case 7 - Differential stress (sun $\perp Z$ spin , A_p = 400) (ΔV > 1000 V).

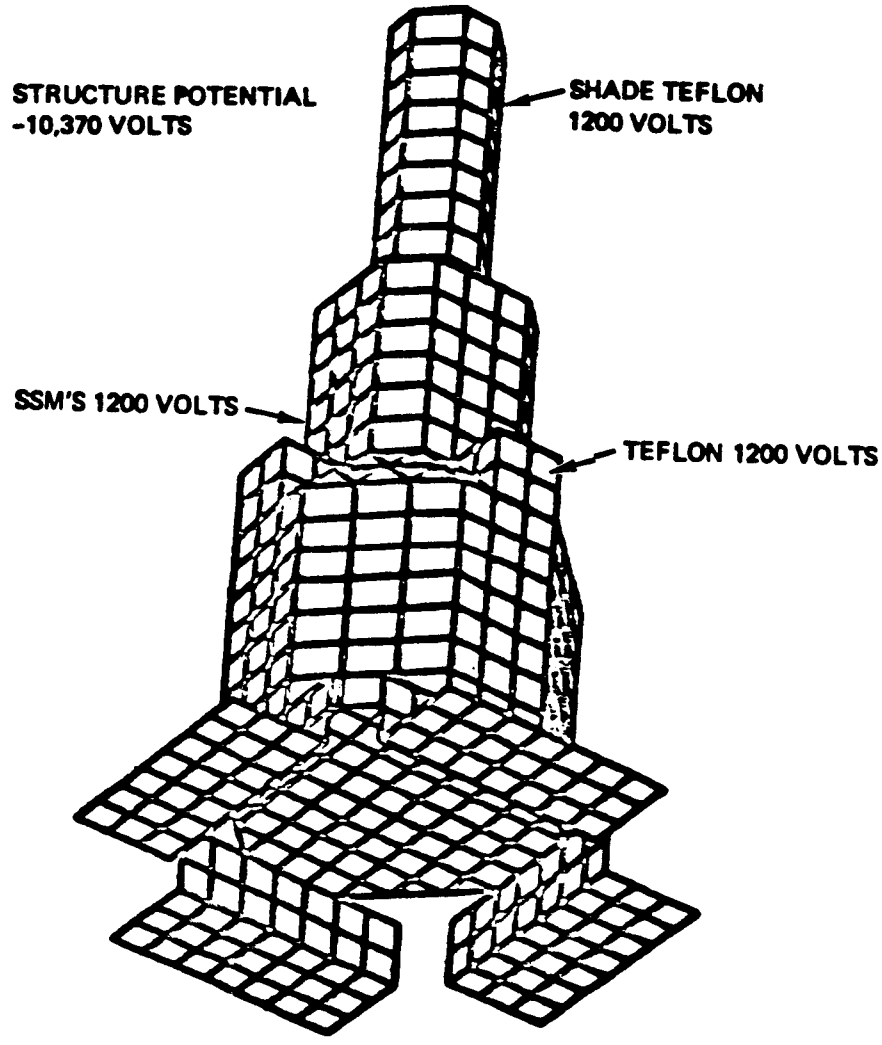

Figure 16. Case 8 - Differential stress (eclipse, A_p = 400) (ΔV > 1000 V).

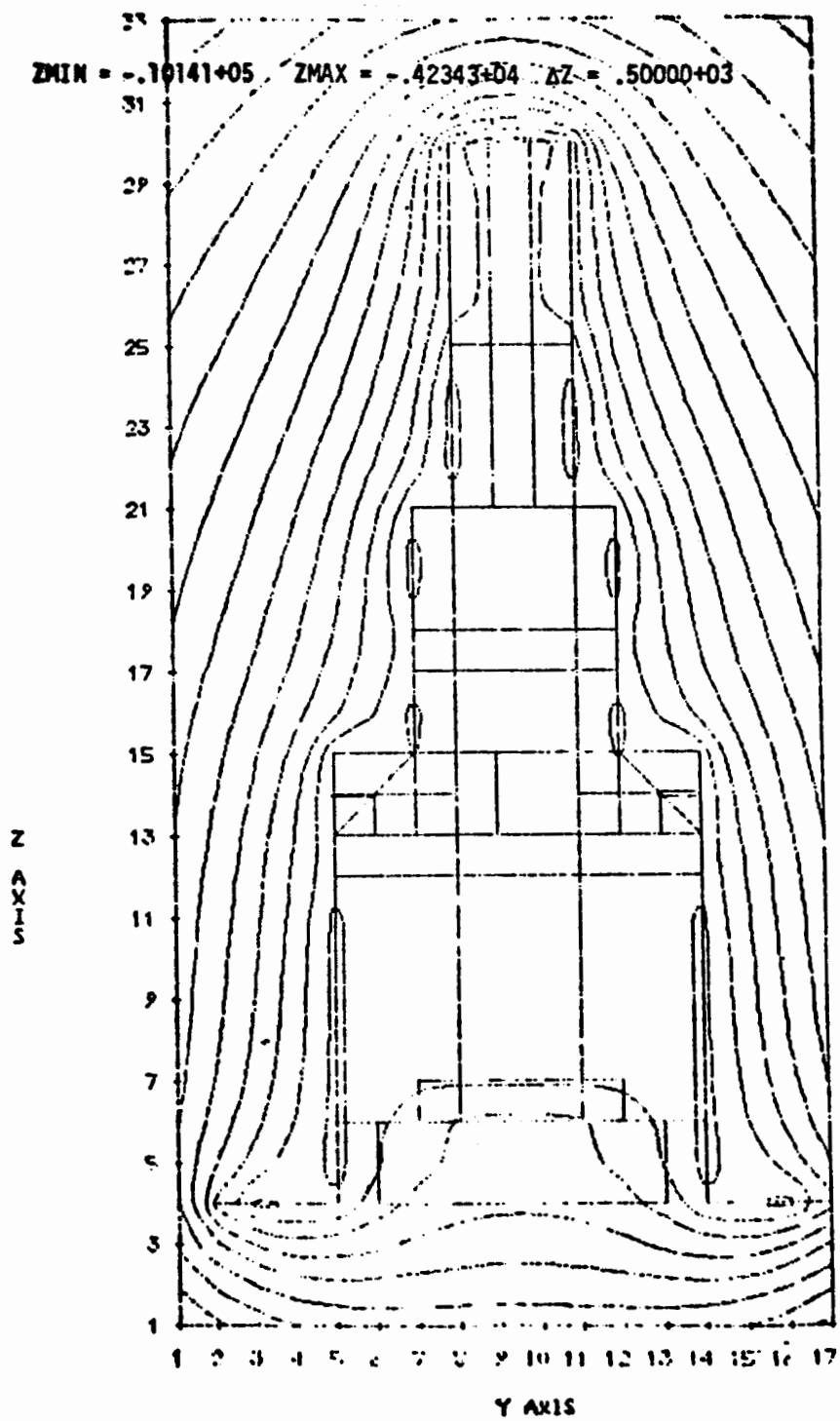

Figure 17. Case 6 (sun -Z, A_p = 400) potential contours along the Y-Z plane of X = 9.

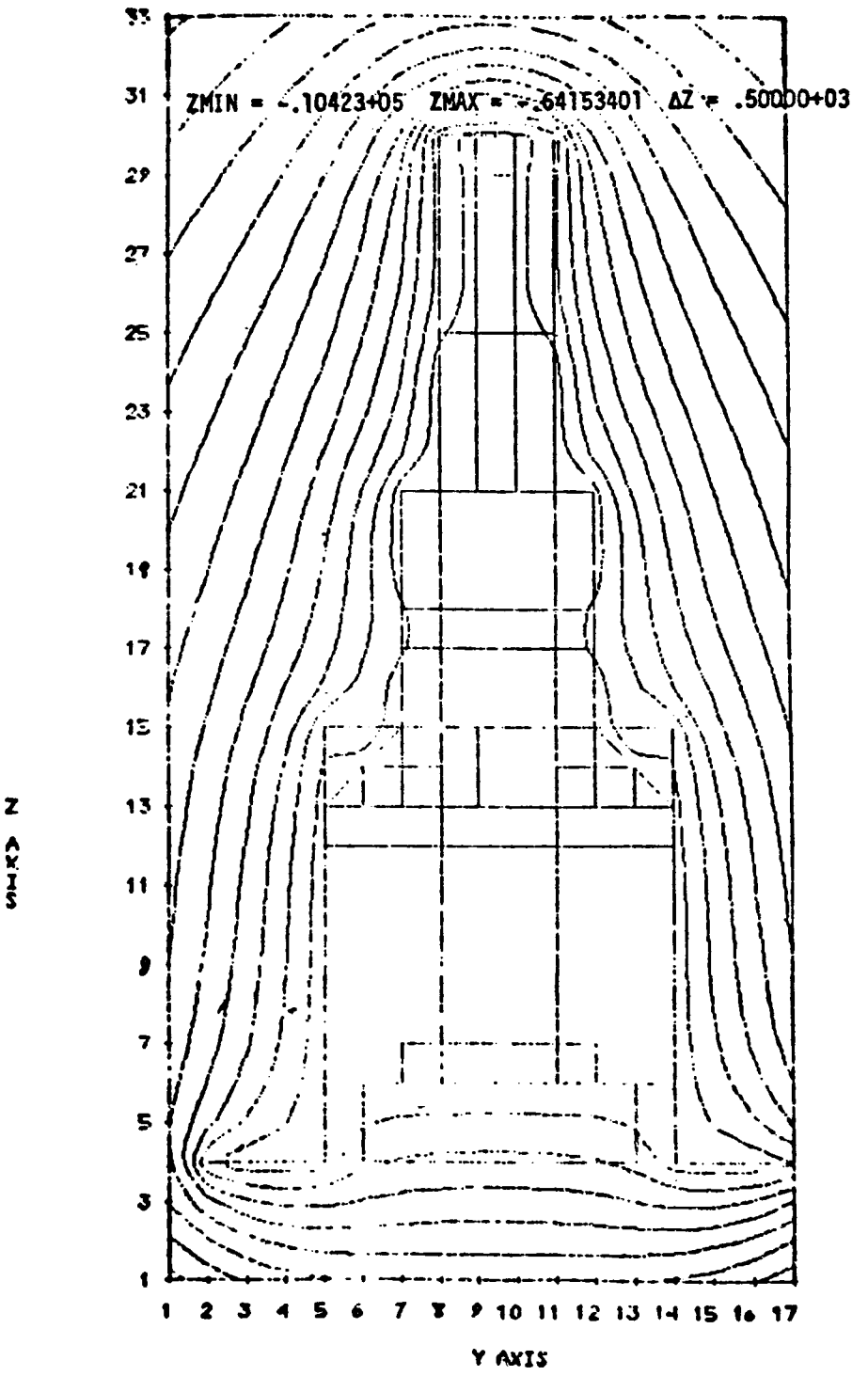

Figure 18. Case 8 (eclipse, A_p = 400) potential contours along the Y-Z plane of X = 9.

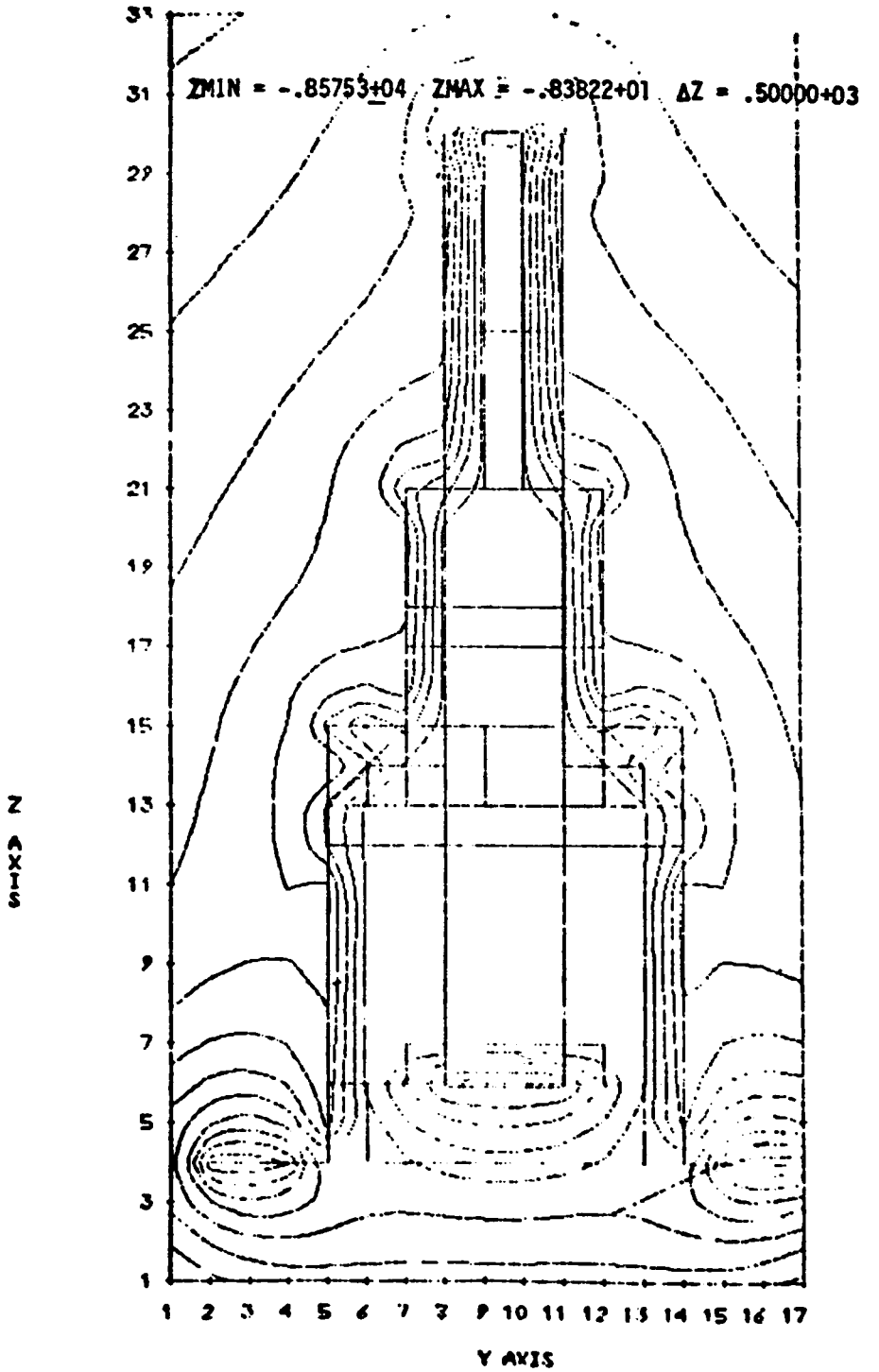

Figure 19. Case 7 (sun $\perp$Z, A_p = 400) potential contours along the Y-Z plane of X = 9.